Iron-based metal organic framework as an effective lead ions remover from aqueous solution: Thermodynamic and kinetic studies

Ntaote David Shooto[1], Ezekiel Dixon Dikio[1], Donbebe Wankasi[1], Lucky Mashudu Sikhwivhilu[2]

[1]*Applied Chemistry and Nano-Science Laboratory, Department of Chemistry, Vaal University of Technology, Vanderbijlpark, South Africa*
[2]*Advanced Materials Division, Mintek, Nanotechnology Innovation Centre, Randburg, South Africa*

Abstract

Metal organic frameworks (MOFs) based on iron as a central metal ion and 1,2,4,5-tetrabenzenecarboxylic acid as ligand was successful synthesized, characterized and studied as adsorbent for the removal of lead ions in aqueous solution. Characterization of Fe-MOF was attained by SEM, EDX, TGA and FT-IR techniques. EDX spectrum showed the presence of C, O and Fe, which may facilitate in creating charges and functionalities on the surface of the Fe-MOF for adsorption. The kinetic and thermodynamic parameters were also investigated. The results showed that Fe-MOF has a high Pb^{2+} adsorption affinity. The removal of Pb^{2+} from aqueous solutions varied with concentration, contact time and temperature. All adsorption studies were carried out in batch experiments.

Keywords: lead, kinetics, adsorption, thermodynamics, metal organic frameworks, synthesis.

Available online at the Journal website: http://www.ache.org.rs/HI/

SCIENTIFIC PAPER

UDC 546.815:544.3/.4:66.081.3

Hem. Ind. **71** (3) 221–229 (2017)

Levels of heavy metals in the environment have increased in the last decades due to rapid industrialization witnessed from 1970 to present day. The presence of heavy metals in the environment is concerning due to the toxic nature of these metals [1]. Heavy metals can be found in the air, soil, water, flesh of animals and also in vegetables. Absorption of heavy metals can cause damage in the human health causing death [2]. Lead is a toxic heavy metal, and mainly used in industries such as metal plating and finishing, printing, photographic materials, explosive manufacturing, ceramic and glass manufacturing. Severe exposure to lead has been connected with sterility, abortion, still-births and neonatal death [3–5]. Hence, there is a crucial need for the development of a method that will effectively remove lead from aqueous solution [6].

Over the years, as heavy metals pollution increased, many techniques have been developed for the treatment of heavy metal contaminated water such as: chemical precipitation [7], ion exchange [8], membrane separation [9], solvent extraction [10], reverse osmosis [11], photo-catalysis [12], floatation [13], etc. These conventional water treatment techniques generally involve some disadvantages such as high reagent or energy requirements, generation of metal bearing sludge or other waste products that require safe disposal [14]. Also, they are cost effective and one of their major drawbacks is the inability to remove metals at low concentration [15,16]. Among these techniques, adsorption has been shown to be a less expensive alternative and more efficient technology for the removal of heavy metals from an aqueous solution [17]. Activated carbon adsorption method is very effective for the removal of heavy metals, but it is more difficult to regenerate, and the processing cost is high [18].

Meta organic frameworks (MOFs) are materials consisting of metal ions (connector) linked together by organic bridging ligands (linker) to create a networked structure with well-defined pores that make them extremely versatile materials [19]. They exhibit high porosity and specific surface area thus; they are extensively applied in catalysis, sensors, separation, and drug delivery [20–23]. Moreover, recently MOFs also show great promise as heavy metals adsorbents in aqueous solution due to their functional groups in the linker and their porous nature. Literature survey shows that few studies have been reported on MOFs as potential heavy metal adsorbents in aqueous solution [24,25]. These materials have not been exploited enough especially in the field of adsorption. Hence, in this research, we report the synthesis of iron organic-framework material, its characterization and potential as an adsorbent for lead ions removal in aqueous solutions.

EXPERIMENTAL

Materials

All reagents were obtained from commercial sources and were used without further purification: *N,N*-Dimethylformamide ($HCON(CH_3)_2$, DMF, 99.8%; AnalaR), iron(III)nitrate nonahydrate ($Fe(NO_3)_3{\cdot}9H_2O$,

Correspondence: N.D. Shooto, Applied Chemistry and Nano-Science Laboratory, Department of Chemistry, Vaal University of Technology, Vanderbijlpark, 1900, South Africa.
E-mail: davidshooto12@gmail.com
Paper received: 20 January, 2016
Paper accepted: 17 June, 2016
https://doi.org/10.2298/HEMIND160120032S

99.95%, Sigma Aldrich), 1,2,4,5-tetrabenzenecarboxylic acid ($C_{10}H_6O_8$, 96%, Sigma-Aldrich), methanol (CH_3OH, 99.9%; Sigma-Aldrich), lead nitrate ($Pb(NO_3)_2$, 99%, Radchem).

Synthesis procedure: Iron metal organic framework (Fe-MOF)

Iron metal organic framework (Fe-MOF) was synthesized by a solvothermal method. DMF (80 mL) was transferred into a round bottom flask, subsequently (0.012 mol) $Fe(NO_3)_3$ and (0.012 mol) 1,2,4,5-tetrabenzenecarboxylic acid were dissolved in it by mild stirring. The solution was refluxed for 2 h at 120 °C while stirring. Ruby red crystals were obtained and isolated using a centrifuge and washed with methanol several times. The obtained crystals were then dried in an air oven at 40 °C for 30 min and used for further experiments.

Lead solution preparation

Pb^{2+} stock solution (100 ppm) was prepared by dissolving 0.1 g $Pb(NO_3)_2$ in 1 L of distilled water. Dilutions were made to 80, 60, 40 and 20 ppm, respectively.

Adsorption procedure

Concentration effect. The Fe-MOF sample (0.1 g) was weighed, and placed into each of the 3 test tubes. Metal ion solution (20 mL) with standard concentrations of 20, 40 and 60 ppm from $Pb(NO_3)_2$ was added to each test tube containing the weighed sample and equilibrated by rocking for 30 min and centrifuged at 2500 rpm for 5 min and decanted. The supernatants were stored for Pb^{2+} analysis.

Adsorption kinetics

Time dependence studies. The Fe-MOF sample (0.1 g) was weighed and transferred into each of the 3 test tubes. Metal ion solution (20 mL) with standard concentration of 60 ppm from $Pb(NO_3)_2$ was added to each test tube containing the weighed sample and equilibrated by agitation for each time intervals of 10, 20 and 30 min, respectively. The powered sample suspension was centrifuged for 5 min at 2500 rpm and decanted. The supernatants were stored for Pb^{2+} analysis.

Temperature effect

The Fe-MOF sample (0.1 g) was weighed and placed in 4 test tubes. Metal ion solution (20 mL) with standard concentration of 60 ppm from $Pb(NO)_3)_2$ was added to each test tube containing the weighed sample and equilibrated by rocking for 30 min at temperatures of 25, 40, 60 and 80 °C, respectively, using water bath. The solution was immediately centrifuged at 2500 rpm for 5 min and then decanted. The supernatant was stored for Pb^{2+} analysis.

Characterization of the adsorbent

The chemical features of the as-prepared Fe-MOF composite were examined by SEM, EDX, XRD, FT-IR and TGA techniques. The surface morphology and EDX measurements were recorded with a JOEL 7500F emission scanning electron microscope. Thermogravimetric analyzer (TGA), TGA analyzer, Perkin Elmer TGA 4000 were used; analyses were performed from 30 to 900 °C at a heating rate of 10 °C/min under a nitrogen atmosphere. Fourier transformed infrared spectroscopy (FT-IR) was performed using Perkin Elmer spectrometer. The measuring range extended from 4000 to 520 cm^{-1}. After adsorption, atomic adsorption spectroscopy (AAS) Shimadzu ASC 7000 auto sampler was used to measure the remaining Pb^{2+} in the solution.

Data analysis

The uptake of heavy metal ions was calculated from the mass balance, which was stated as the amount of solute adsorbed onto the solid. Mathematically can be expressed in Eq. (1) [19]:

$$q_e = \frac{(c_o - c_e)}{S} \tag{1}$$

where q_e is heavy metal ions concentration adsorbed on adsorbent at equilibrium (mg of metal ion/g of adsorbent), c_o is initial concentration of metal ions in the solution (ppm), c_e is equilibrium concentration or final concentration of metal ions in the solution (ppm) and S is dosage concentration and it is expressed by Equation (2):

$$S = \frac{v}{m} \tag{2}$$

where v is the initial volume of metal ions solution used (in L) and m is the mass of adsorbent (in g).

The adsorption percent was also calculated using Eq. (3):

$$\%\ \text{Adsorption} = 100\frac{c_o - c_e}{c_o} \tag{3}$$

Equilibrium studies

Langmuir plots were carried out using the linearized Equation (4) below

$$\frac{M}{X} = \frac{1}{abc_e} + \frac{1}{b} \tag{4}$$

where X is the quantity of Pb^{2+} sorbed per mass M of the MOF in mg/g, a and b are the Langmuir constants obtained from the slope and intercepts of the plots.

Langmuir isotherm was shown in terms of an equation of separation factor or equilibrium parameter S_f (5) [26]:

$$S_f = \frac{1}{1+ac_o} \quad (5)$$

The value of the parameter S_f provides an indication of the type of sorption isotherm. If $S_f > 1.0$, the sorption isotherm is unfavourable; $S_f = 1.0$ (linear); $0 < S_f < 1.0$ (favourable) and $S_f = 0$ (irreversible).

The level of sorption of the Pb^{2+} in the MOF was measured from the Freundlich plots applying the linearized Eq. (6):

$$\ln\frac{x}{M} = \frac{1}{n}\ln c_e + \ln k \quad (6)$$

where K and n are Freundlich constants and $1/n$ is approximately equal to the adsorption capacity.

The fraction of the MOF surface covered by Pb^{2+} was calculated using Eq. (7):

$$\theta = 1 - \frac{c_e}{c_o} \quad (7)$$

with θ as degree of surface coverage

Thermodynamics studies

The capability of the adsorbent to reduce the amount of Pb^{2+} in solution was evaluated by the number of cycles of equilibrium sorption process needed according to the value of the partition coefficient (K_d) in Eq. (8) [27]:

$$K_d = \frac{c_{ads}}{c_{aq}} \quad (8)$$

where c_{aq} is the concentration of Pb^{2+} (mg/g) in solution; c_{ads} is concentration of Pb^{2+} ppm in MOF.

The isosteric heat of adsorption at constant surface coverage is calculated using the Clausius–Clapeyron Equation (9):

$$\frac{\mathrm{d}(\ln c_e)}{\mathrm{d}T} = \frac{\Delta H^*}{RT^2} \quad (9)$$

where ΔH^* is the isosteric heat of adsorption (kJ/mol), R is the ideal gas constant (8.314 J/(mol K)), and T is temperature (K). Integrating the above equation, assuming that the isosteric heat of adsorption is temperature independent, gives the following equation:

$$\ln c_e = -\frac{\Delta H^*}{R}\frac{1}{T} + K \quad (10)$$

where K is a constant.

The isosteric heat of adsorption is calculated from the slope of the plot of ln c_e *versus* $1/T$.

The linear form of the modified Arrhenius equation was applied to the experimental data to measure the sticking probability (S^*) and activation energy (E_a) in Eq. (11) [28]:

$$In(1-\theta) = S^* + \frac{E_a}{RT} \quad (11)$$

The Gibbs free energy ($\Delta G°$) of the adsorption was applied to evaluate the spontaneity of the process using the Eq. (12):

$$\Delta G^\circ = -RT\ln K_d \quad (12)$$

where K_d is derived from Eq. (8).

Further examination was done to measure the enthalpy ($\Delta H°$) and entropy ($\Delta S°$) of sorption by using Eq. (13):

$$\Delta G^\circ = \Delta H^\circ - T\Delta S^\circ \quad (13)$$

The probability of an adsorbate finding a vacant site on the adsorbent surface during sorption may be correlated by the number of hopping (n) done by the adsorbate as shown in Eq. (14):

$$n = \frac{1}{(1-\theta)\theta} \quad (14)$$

Kinetic studies

To determine the kinetic compliance of the experimental data, the results were analyzed with the following kinetic models:

Zero-order kinetic model,

$$q_t = q_o + k_o t \quad (15)$$

where q_e and q_t are the amounts of the adsorbed metal ion (mg/g) at the equilibrium time and at any instant of time t, respectively, and k_o is the rate constant of the zero-order adsorption operation. Plotting of q_t *versus* t gives a straight line for the zero-order kinetics.

First-order kinetic model,

$$\ln q_t = \ln q_o + k_1 t \quad (16)$$

where k_1 is the rate constant. Plotting of ln q_t *versus* t gives a straight line for the first-order kinetics.

Second-order kinetic model,

$$\frac{1}{q_t} = \frac{1}{q_o} + k_2 t \quad (17)$$

where k_2 (1/min) is the rate constant. Plotting of $1/q_t$ *versus* t gives a straight line for the second-order kinetics.

RESULTS AND DISCUSSION

SEM micrographs of Fe-MOF are shown in Figure 1a and b. Figure 1a shows SEM image taken at 140× magnification and Figure 1b 300× magnification. The images

indicated that the as-prepared MOF is primarily constituted of small crystalline material of irregular shapes and sizes. Because of the smallness of the particle size, we anticipate high adsorption rate for this material.

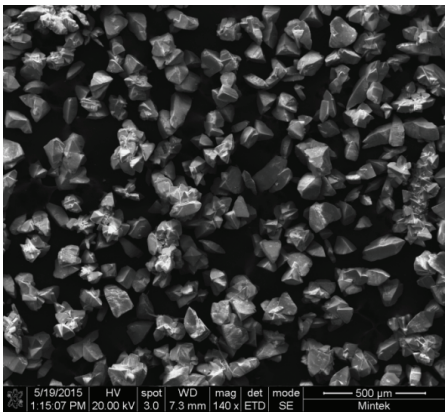

(a)

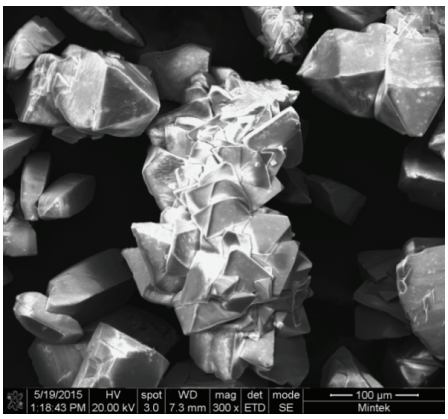

(b)

Figure 1. Scanning electron micrograph images of synthesized iron metal organic framework obtained from iron(III) nitrate reacted with 1,2,4,5-tetrabenzenecarboxylic acid.

Elemental analysis of the as-prepared Fe-MOF sample was investigated. The EDX spectrum in Figure 2 showed the presence of C, O and Fe as distinct peaks. The at.%) of these elements is as follows: C (67.7%), O (25.2%) and Fe (7.1%) as presented in Table 1. The presence of these elements confirms the successful synthesis of Fe-MOF and these elements will create charges on the surface of the as-prepared Fe-MOF and result in electrostatic forces between the sample and Pb^{2+} in the solution.

To examine the thermal stability and to determine the weight loss of the MOF composite taking place in an inert atmosphere, TGA and DTA analyses were carried out as shown in Figure 3. The plots showed multiple decomposition steps. First decomposition was observed between 33–157 °C as confirmed by DTA plot. This corresponds to the release of guest molecules such as physically adsorbed moisture, water molecules, methanol that was introduced during washing and organic solvent material DMF trapped in the cages of Fe-MOF. Second decomposition was observed between 177–556 °C as shown by DTA plot. This weight loss corresponds to the disintegration of Fe-MOF, first it lost its side bonds; hydrogen and oxygen bonds between Fe-MOF molecules; instantly followed by the breaking down of main bonds (Fe–O) within Fe-MOFs. Third decomposition as confirmed by DTA plot to be between 572–662 °C, it was pyrolysis and iron oxidation state changed from Fe^{3+} to Fe^{2+} then Fe. Beyond 663 °C, there is no weight change.

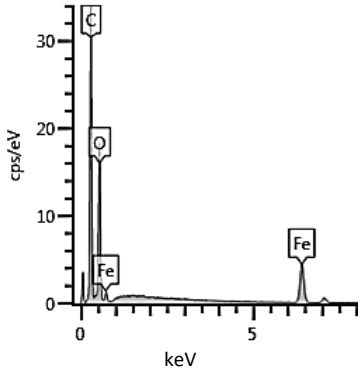

Figure 2. Energy dispersive X-ray spectroscopy (EDX) of synthesized iron metal organic framework obtained from iron(III) nitrate reacted with 1,2,4,5-tetrabenzenecarboxylic acid.

Table 1. Table of percentage weight of element and atom obtained from energy dispersive spectroscopy of iron metal organic framework

Element	Content, at.%
Carbon	67.7
Oxygen	25.2
Iron	7.1
Total	100.0

Infrared spectrum of iron metal-organic framework in the wavenumber region between 650 and 4000 cm^{-1} is shown in Figure 4. Very broad band located at 3038 cm^{-1} is assigned to O–H group which indicates the presence of loosely bound water molecules in the Fe--MOF. The strong absorption peak near 1709 cm^{-1} can be assigned to the C=O stretching vibration in the 1,2,4,5-tetrabenzenecarboxylic acid. Strong bands at 1594 and 1497 cm^{-1} are attributed to asymmetric and symmetric stretching vibration of carbonyl groups, respectively [29]. Bending vibration of (Fe–O) presents a band at 654 cm^{-1}. Other importance peaks are the stretching C–O and bending O–H vibrational frequencies seen at 1332 and 1390 cm^{-1}, respectively, indicating the presence of a carboxylic acid group. These results suggest that Fe-MOF was successfully synthe-

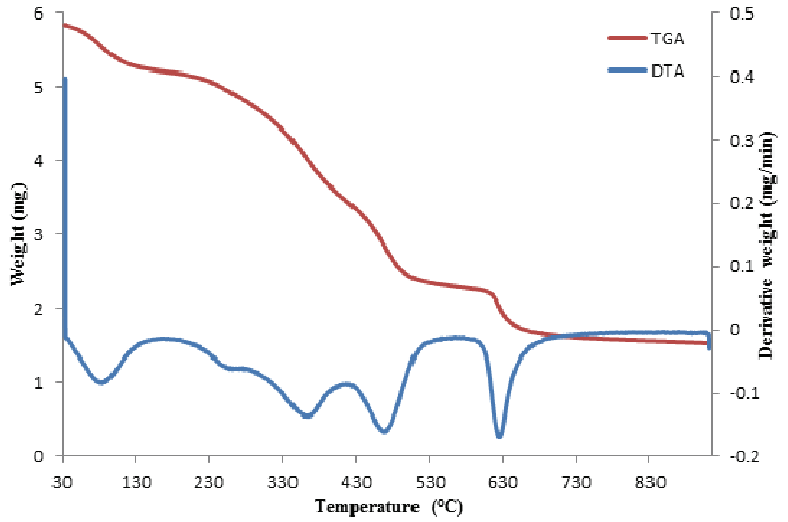

Figure 3. Thermalgravimetric analysis (TGA) and derivative thermogravimetric analysis (DTA) of iron metal organic framework.

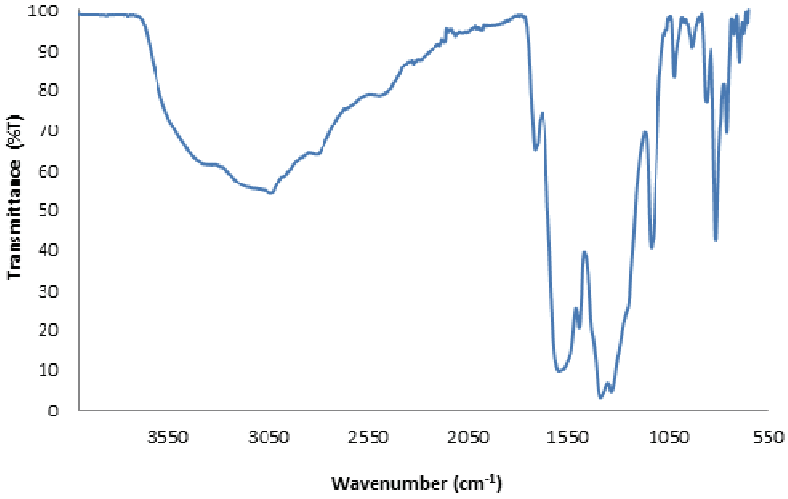

Figure 4. Fourier transform infrared (FT-IR) spectra of synthesized iron metal organic framework.

sized by the iron ions and 1,2,4,5-tetrabenzenecarboxylic acid organic ligands.

The effect of temperature on Pb^{2+} adsorption to Fe--MOF was investigated at different temperatures 25, 40, 60 and 80 °C as shown in Figure 5. It is observed that there was a rapid adsorption from 0–25 °C after which as temperature increased there was a slight improvement in amount adsorbed. Subsequently this suggests that there was a creation of new adsorption sites or the increased rate of intra-particle diffusion adsorbate into the pores of the Fe-MOF at higher temperatures. This could also be due to the easy mobility of Pb^{2+} from the bulk solution towards the adsorbent surface, which tends to enhancethe accessibility to the adsorbent active sites. Thus, the high temperature favours the adsorption of Pb^{2+} on Fe-MOF.

Isosteric heat of adsorption ΔH_x is one of the basic requirements for the characterization and optimization of an adsorption process and is a critical design variable in estimating the performance of an adsorptive separation process. Knowledge of the heats of sorption is very important for equipment and process design. A plot of ln c_e against $1/T$ in Figure 6 gives a slope equal to ΔH_x. Below 80 kJ/mol is physical adsorption and between 80–400 kJ/mol is chemical adsorption [30––32]. The value of ΔH_x derived from equation 10 was 142.2 kJ/mol which indicates that adsorption mechanism was chemical adsorption.

The activation energy E_a and the sticking probability S^* were calculated by Eq. (11). The value shown in Table 2 for E_a and S^* are –20.45 kJ/mol and 0.1186, respectively, as shown in Figure 7. Activation energy, E_a, values indicate that very low energy was required to initiate the sorption thus the sorption process is exothermic. The sticking probability S^* indicates the measure of the potential of an adsorbate to remain on the adsorbent. It is often interpreted as $S^* > 1$ (no sorption), $S^* = 1$ (mixture of physic-sorption and chemisorp-

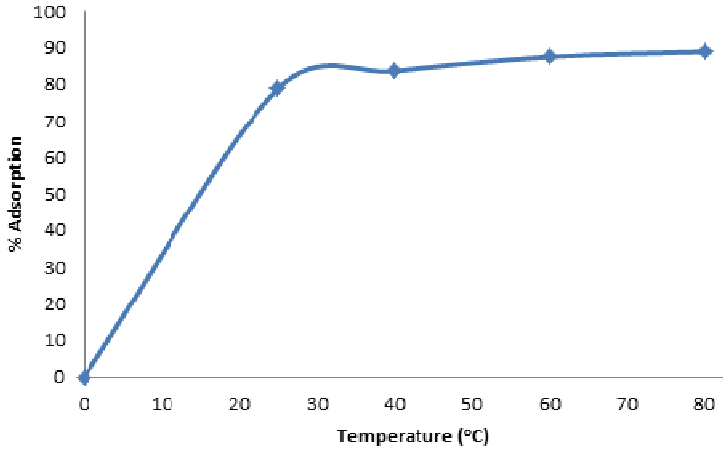

Figure 5. Temperature effect on adsorption of Pb^{2+} onto metal organic framework.

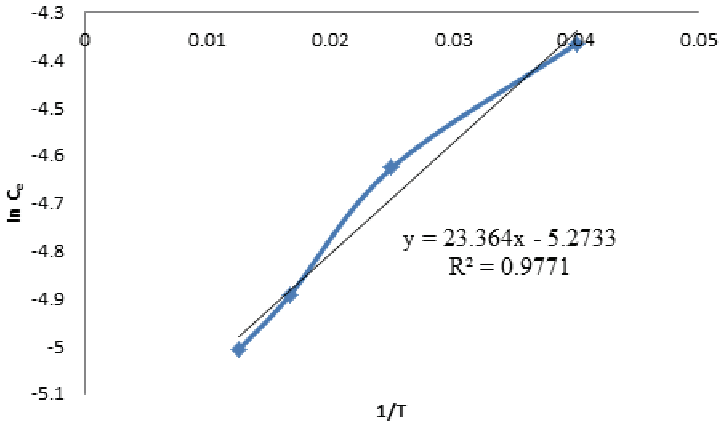

Figure 6. Plot of ln c_e vs. 1/T for adsorption of Pb^{2+} onto metal organic framework.

tion), $S^* = 0$ (indefinite sticking – chemisorption), $0 < S^* < 1$ (favourable sticking–physisorption).

The probability of Pb^{2+} finding vacant site on the surface of the MOF during the sorption was correlated by the number of hopping (n) done by the Pb^{2+}. It is calculated by Eq. (14). The obtained hopping number was 10. The lower the hopping number, the faster the adsorption. The low value of *n* obtained in this study suggests that the adsorption of Pb^{2+} on the MOF was very fast.

Table 2 also presents the Gibbs free energy $\Delta G°$ for the sorption of Pb^{2+} by the Fe-MOF which was calculated by Eq. (12). Gibbs free energy is the fundamental criterion of spontaneity. The obtained values of $\Delta G°$ indicate that the sorption process was spontaneous. The values of the enthalpy change ($\Delta H°$) and entropy change ($\Delta S°$) were calculated using Eq. (13) to be 3.82 kJ/mol and 20.9 J/(mol K), respectively as shown in Figure 8. A plot of $\Delta G°$ against temperature gives a straight line graph with slope and intercept defining the $\Delta H°$ and $\Delta G°$. A positive $\Delta H°$ suggests that sorption proceeded favourably at higher temperature and the sorption mechanism was endothermic.

Figure 9 shows the influence of contact time at (10, 20 and 30 min) on the adsorbed Pb^{2+}. The adsorption rates increased steadily at the beginning, probably due to the readily accessible sites on the adsorbent surface. As the surface adsorption sites became saturated, the uptake rate was slowed down and controlled by the transport rate from the exterior to the interior sites of the adsorbent.

Table 2. Thermodynamic parameters of the adsorption of Pb^{2+} onto Fe-MOF

T, K	$-\Delta G°$ / kJ mol^{-1}	$\Delta H°$ / kJ mol^{-1}	$\Delta S°$ /kJ mol^{-1} K^{-1}	E_a / kJ mol^{-1}	ΔH_x / kJ mol^{-1}
298	2.817	3.82	20.9	–20.45	142.2
313	3.051				
333	3.246				
353	3.441				

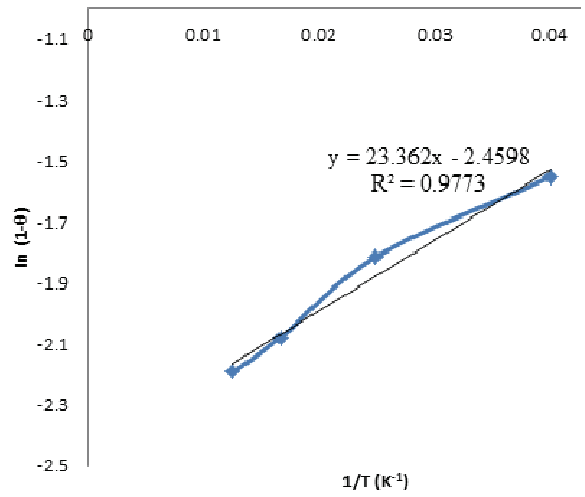

Figure 7. Plot of ln (1–θ) vs. 1/T for adsorption of Pb^{2+} onto metal organic framework.

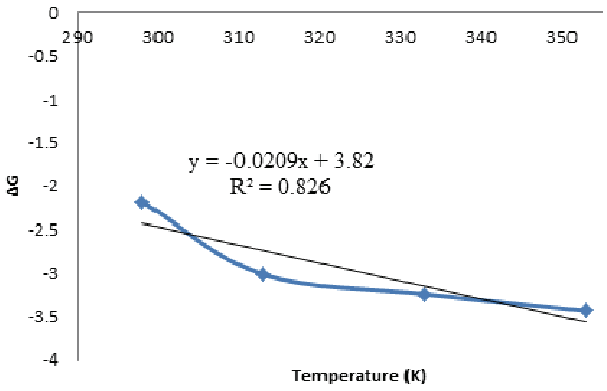

Figure 8. Plot of ΔG vs. T for adsorption of Pb^{2+} onto metal organic framework.

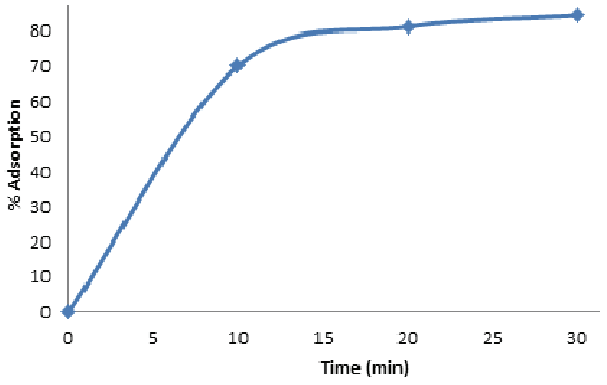

Figure. 9. Effect of contact time on adsorption of Pb^{2+} onto metal-organic framework.

The experimental data fitted only zero-order kinetic model as it gave a straight line (R^2 = 0.9995). First-order kinetic and second-order kinetic models give (R^2 of 0.9891 and 0.9693, respectively) as shown in Figures 10–12.

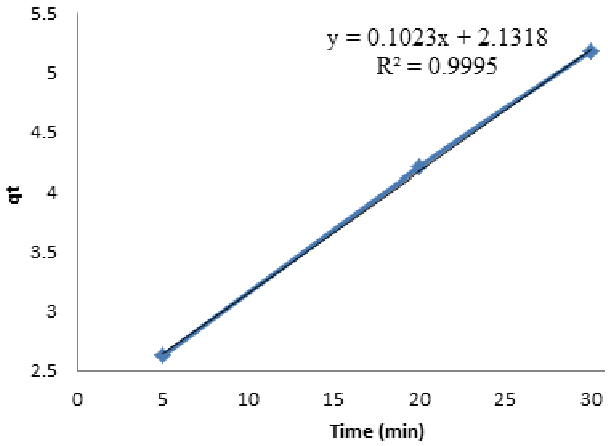

Figure 10. Plot of q_t vs. t for adsorption of Pb^{2+} onto metal organic framework.

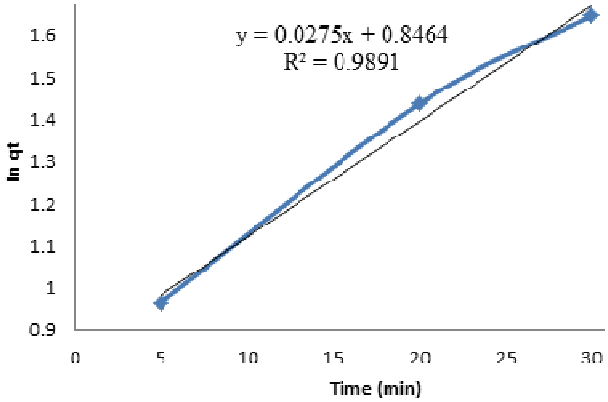

Figure 11. Plot of ln q_t vs. t for adsorption of Pb^{2+} onto metal organic framework.

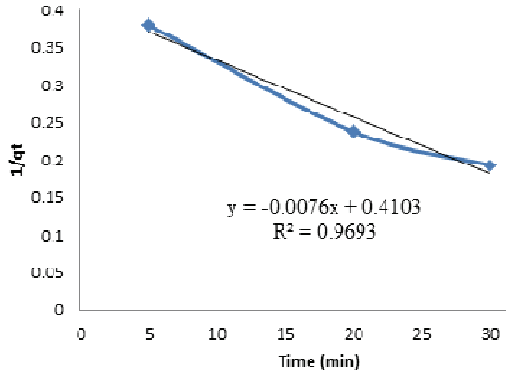

Figure 12. Plot of $1/q_t$ vs. t for adsorption of Pb^{2+} onto metal organic framework.

The percentage sorption by Fe-MOF at different Pb^{2+} concentrations (20, 40 and 60 ppm) is presented in Figure 13. The maximum adsorption of 85.31% took place at concentration of 60 ppm Pb^{2+}. This is because at lower concentration more MOF pore spaces were available for the Pb^{2+} but as the concentration of Pb^{2+} increased, the adsorption capacity of the MOF dec-

reased due to reduced availability of free pore spaces and active sites.

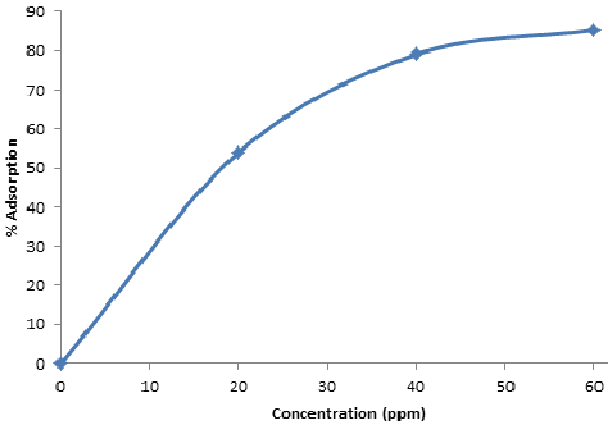

Figure 13. Concentration effect on adsorption of Pb^{2+} onto metal organic framework.

In determining the nature of the adsorption process, whether favourable or unfavourable, the dimensionless constant separation term S_f was investigated (Eq. (5)). The obtained result (S_f = 0.8156) which showed that the sorption of Pb^{2+} onto the Fe-MOF was favourable.

CONCLUSION

In this work, a highly crystalline Fe-MOF material has been synthesized using a solvothermal method. The characterization of Fe-MOF material was confirmed by SEM, FT-IR, TGA and XRD. The proposed route of using Fe-MOF as Pb^{2+} adsorbent demonstrated great potential. Thermodynamics and kinetic batch adsorption studies recorded rapid and effective uptake of the Pb^{2+} by the Fe-MOF. The adsorption was favoured at high temperature and energy which was endothermic with both physisorption and chemisorption mechanisms. The results from this study will add to the knowledge base on the synthesis, characterization and the use of metal organic frameworks for the sorption studies.

Acknowledgements

This work was supported by a research grant from the Faculty of Applied and Computer Science Research and Publications Committee of Vaal University of Technology.

REFERENCES

[1] T.K. Naiya, A.K. Bhattacharya, S. Mandal, S.K. Das, The sorption of lead (II) ions on rice husk ash, J. Hazard. Mater. **163** (2009) 1254–1264.

[2] R. Ayyappan, A.C. Sophia, K. Swaminathan, S. Sandhya, Removal of Pb(II) from aqueous solution using carbon derived from agricultural wastes, Process Biochem. **40** (2005) 1293–1299.

[3] J. Goel, K. Kadirvelu, C. Rajagopal, V.K. Garg, Removal of lead (II) by adsorption using treated granular activated carbon: batch and column studies, J. Hazard. Mater. **125** (2005) 211–220.

[4] B.L. Martins, C.C.V. Cruz, A.S. Luna, C.A. Henriques, Sorption and desorption of Pb $^{2+}$ ions by dead Sargassum sp. biomass, Biochem. Eng. J. **27** (2006) 310–314.

[5] S. Tunali, T. Akar, A.S. Ozcan, I. Kiran, A. Ozcan, Equilibrium and kinetics of biosorption of lead(II) from aqueous solutions by Cephalosporium aphidicola, Sep. Purif. Technol. **47** (2006) 105–112.

[6] L. Largitte, J. Laminie, Modelling the lead concentration decay in the adsorption of lead onto a granular activated carbon, J. Environ. Chem. Eng. **3** (2015) 474–481.

[7] R. Kumar, P. Pal, Response surface-optimized Fenton's pre-treatment for chemical precipitation of struvite and recycling of water through downstream nanofiltration, Chem. Eng. J. **210** (2012) 33–44.

[8] Y.C. Lai, Y.R. Chang, M.L. Chen, Y.K. Lo, J.Y. Lai, D.J. Lee, Poly(vinyl alcohol) and alginate cross–linked matrix with immobilized Prussian blue and ion exchange resin for cesium removal from waters, Bioresour. Technol. **214** (2016) 192–198.

[9] J. Zhang, H. Yu, X. Quan, S. Chen, Y. Zhang, Ceramic membrane separation coupled with catalytic ozonation for tertiary treatment of dyestuff wastewater in a pilot-scale study, Chem. Eng. J. **301** (2016) 19–26.

[10] G. Pandey, S. Mukhopadhyay, A.U. Renjith, J.M. Joshi, K.T. Shenoy, Recovery of Hf and Zr from slurry waste of zirconium purification plant using solvent extraction, Hydrometallurgy **163** (2016) 61–68.

[11] J.N. Hakizimana, B. Gourich, C. Vial, P. Drogui, A. Oumani, J. Naja, L. Hilali, Assessment of hardness, microorganism and organic matter removal from seawater by electrocoagulation as a pre–treatment of desalination by reverse osmosis, Desalination **393** (2016) 90–101.

[12] E. Diaz, M. Cebriana, A. Bahamonde, M. Faraldos, A. F. Mohedano, J. A. Casas, J. J. Rodriguez, Degradation of organochlorinated pollutants in water by catalytic hydrodechlorination and photocatalysis, Catal. Today **266** (2016) 168–174.

[13] S. Walker, R. M. Narbaitz, Hollow fiber ultrafiltration of Ottawa River water: Floatation versus sedimentation pre-treatment, Chem. Eng. J. **288** (2016) 228–237.

[14] N. Tewari, P. Vasudevan, B.K. Guha, Study on biosorption of Cr(VI) by Mucor hiemalis, Biochem. Eng. J. **23** (2005) 185–192.

[15] C.F. Brasquet, K. Kadirvelu, P.L. Cloirec, Removal of metal ions from aqueous solution by adsorption onto activated carbon cloths: adsorption competition with organic matter, Carbon **40** (2002) 2387–2392.

[16] N.R. Bishnoi, M. Bajaj, N. Sharma, A. Gupta, Adsorption of Cr(VI) on activated rice husk carbon and activated alumina, J. Bioresour. Technol. **91** (2004) 305–307.

[17] X.H. Do, B.K. Lee, Removal of Pb^{2+} using a biochar-alginate capsule in aqueous solution and capsule regeneration, J. Environ. Manage. **131** (2013) 375–382.

[18] A. Kundu, G. Redzwan, J.N. Sahu, S. Mukherjee, B.S. Gupta, M.A. Hashim, *Hexavalent chromium adsorption by a novel* activated carbon prepared by microwave activation, Bioresour. **9** (2014) 1498–1518.

[19] L.F. Marques, C.C. Correa, S.J.L. Ribeiro, M.V.D. Santos, J.D.L. Dutra, R.O. Freire, F.C. Machado, Synthesis, structural characterization, luminescent properties and theoretical study of three novel lanthanide metal–organic frameworks of Ho(III), Gd(III) and Eu(III) with 2,5-thiophenedicarboxylate anion, J. Solid State Chem. **227** (2015) 68–78.

[20] A. Dhakshinamoorthy, M. Alvaro, H. Garcia, Aerobic oxidation of styrenes catalyzed by an iron metal organic framework, A.C.S. Catal. **1** (2011) 836–840.

[21] R.C. Huxford, J.D. Rocca, W. Lin, Metal-organic frameworks as potential drug carriers, Curr. Opin. Chem. Biol. **14** (2010) 262–268.

[22] C. Petit, B. Levasseur, B. Mendoza, T. Bandosz, Reactive adsorption of acidic gases on MOF/graphite oxide composites, J. Microporous Mesoporous Mater. **154** (2012) 107–112.

[23] Y. Yu, X.M. Zhang, J.P. Ma, Q.K. Liu, P. Wang, Y.B. Dong, Cu(I)-MOF: naked-eye colorimetric sensor for humidity and formaldehyde in single-crystalto-single-crystal fashion, Chem. Commun. **50** (2014) 1444–1446.

[24] N. Bakhtiari, S. Azizian, S.M. Alshehri, N.L. Torad, V. Malgras, Y. Yamauchi, Study on adsorption of copper ion from aqueous solution by MOF-derived nanoporous carbon, Microporous Mesoporous Mater. **217** (2015) 173–177.

[25] A. Maleki, B. Hayati, M. Naghizadeh, S.W. Joo, Adsorption of hexavalent chromium by metal organic frameworks from aqueous solution, J. Ind. Eng. Chem. **28** (2015) 211–216.

[26] K.H. Chu, M.A. Hashim, Desorption of Copper from Polyvinyl Alcohol-Immobilized Seaweed Biomass, Acta Biotechnol. **21** (2001) 295–306.

[27] V.J.P. Poots, G. Mckay, J.J. Healy, Removal of Basic Dye from Effluent Using Wood as an Adsorbent, J. Water. Res. **10** (1978) 1067–1070.

[28] D. Wankasi, M. Horsfall, A.I. Spiff, Sorption kinetics of Pb^{2+} and Cu^{2+} ions from aqueous solution by Nipah palm (Nypa fruticansWurmb) shoot biomass, Chem. Tech. J. **9** (2006) 587–592.

[29] D. Wankasi, Adsorption, A Guide to Experimental Data Analysis, Ano Publication Company, Nigeria, 2013, pp. 40–43.

[30] M. Mazaj, G. Mali, M. Rangus, E. Zunkovic, V. Kaucic, N.Z. Logar, Spectroscopic studies of structural dynamics induced by heating and hydration: a case of calcium terephthalate metal-organic framework, J. Phys. Chem. **117** (2013) 7552–7564.

[31] P.N. Palanisamy, A. Agalya, P. Sivakumar, Polymer composite a potential biomaterial for the removal of reactive dye, E. J. Chem. **9** (2012) 1823–1834.

[32] Y. Pei, X. Chen, D. Xiong, S. Liao, G. Wang, Removal and recovery of toxic silver ion using deep-sea bacterial generated biogenic manganese oxides, PLoS One **8** (2013), e81627; doi: 10.1371/journal.pone.0081627.

IZVOD

METALNO ORGANSKO JEDINJENJE NA BAZI GVOŽĐA KAO EFIKASAN ADSORBENS ZA UKLANJANJE JONA OLOVA IZ VODENIH RASTVORA: TERMODINAMIČKA I KINETIČKA ISPITIVANJA

Ntaote David Shooto[1], Ezekiel Dixon Dikio[1], Donbebe Wankasi[1], Lucky Mashudu Sikhwivhilu[2]

[1]*Applied Chemistry and Nano-Science Laboratory, Department of Chemistry, Vaal University of Technology, Vanderbijlpark, South Africa*
[2]*Advanced Materials Division, Mintek, Nanotechnology Innovation Centre, Randburg, South Africa*

(Naučni rad)

Metalno organsko jedinjenje (MOFs) na bazi gvožđa kao centralnog jona i 1,2,4,5-tetrabenzenkarboksilne kiseline kao liganda bio je uspešno sintetisan, okarakterisan i proučavan kao adsorbens za uklanjanje jona olova iz vodenih rastvora. Karakterizacija Fe-MOF je postignuta korišćenjem SEM, EDX, TGA i FT-IR tehnika. EDX spektar pokazuje prisustvo C, O i Fe koji mogu olakšati stvaranje naelektrisanja i funkcionalnih grupa na površini Fe-MOF za proces adsorpcije. Kinetički i termodinamički parametri su takođe ispitivani. Rezultati su pokazali da Fe-MOF ima visoki afinitet adsorpcije prema Pb^{2+}. Uklanjanje Pb^{2+} iz vodenih rastvora zavisi od koncentracije, vremena kontakta i temperature. Svi eksperimenti adsorpcije rađeni su u diskontinualnim sistemima.

Ključne reči: Olovo • Kinetika • Adsorpcija • Termodinamika • Metal-organski materijali • Sinteza